

Symmetry breaking and manipulation of nonlinear optical modes in an asymmetric double-channel waveguide

Rujiang Li¹, Fei Lv¹, Lu Li^{1*} and Zhiyong Xu²

¹*Institute of Theoretical Physics, Shanxi University, Taiyuan 030006, China and*

²*Nonlinear Physics Centre, Research School of Physics and Engineering,
The Australian National University, Canberra ACT, 0200, Australia*

We study light beam propagation in a nonlinear coupler with an asymmetric double-channel waveguide, and derive various analytical forms of optical modes. The results show that the symmetry-preserving modes in a symmetric double-channel waveguide is deformed due to the asymmetry of the two-channel waveguide, and such a coupler supports yet the symmetry-breaking modes. The dispersion relations reveal that the system with self-focusing nonlinear response supports the degenerate modes, while for self-defocusing medium the degenerate modes do not exist. Furthermore, nonlinear manipulation is investigated by launching optical modes supported in double-channel waveguide into a nonlinear uniform medium.

PACS numbers: 42.65.Tg, 42.65.Jx, 42.65.Wi

I. INTRODUCTION

Propagation of optical waves in waveguide arrays has become an important and effective means to investigate various optical phenomena which have analogues in many fields of physics [1]. Special attention has been paid to nonlinear surface waves and nonlinear guided waves in planar layered structures [2–13] and nonlinear couplers [14–18], generation and properties of solitons in nonlinear waveguide arrays [19–24] and other nonlinear periodic systems, such as optically induced lattices [25–28]. The investigation of light beam propagation in waveguide arrays attracts increasing attention due to their potential applications in all-optical signal processing in fiber optic networks and devices, the passive mode-locking by using waveguide array [29], and the beam steering [30–32].

The behavior of light beam propagation in a coupler composed by two-channel nonlinear waveguide gained particular attention because it can exhibit some of universal properties in nonlinear periodic systems and nonlinear waveguide arrays [33]. It is shown that the coupler can support the symmetry-preserving solutions which have the linear counterparts and the symmetry-breaking solutions without any linear counterparts [34–36], in which the spontaneous symmetry-breaking has been experimentally demonstrated in optically induced lattices with a local double-well potential [34].

In this paper, we consider light beam propagation in an asymmetric double-channel waveguide with Kerr-type nonlinear response, and derive various analytical stationary solutions in detail. It is found that the asymmetric double-channel waveguide can break the symmetric form of the symmetry-preserving modes otherwise in the symmetric double-channel waveguide, and such a coupler supports the symmetry-breaking modes. We also inves-

tigate how the type of nonlinear response affects the existence and properties of nonlinear optical modes in the asymmetric double-channel waveguide. The dispersion relation shows that the degenerate modes exist in the system with self-focusing nonlinear response, while for the coupler with self-defocusing response the degenerate modes do not exist. In addition, based on these optical modes supported in asymmetric double-channel waveguide we demonstrate the control and manipulation of optical modes in different nonlinear media by tuning the waveguide parameters.

The paper is organized as follows. In Section II, the model equation describing beam propagation in a double-channel waveguide is derived. In Section III, various analytical forms of optical modes are presented both in self-focusing and self-defocusing media. Meanwhile, the dispersion relations between the total energy and the propagation constant are discussed. In Section IV, we study the nonlinear manipulation of optical modes in double-channel waveguide. The conclusion is summarized in Section V.

II. MODEL EQUATION AND REDUCTIONS

We consider a planar graded-index waveguide with refractive index

$$n(z, x) = F(x) + n_2 I(z, x). \quad (1)$$

Here the first term on the right hand side presents a two-channel waveguide with the different refractive index, namely, $F(x) = n_{11}$ as $-L_0/2 - D_0 < x < -L_0/2$, and $F(x) = n_{12}$ as $L_0/2 < x < L_0/2 + D_0$, otherwise, $F(x) = n_0$ ($< n_{11}, n_{12}$), where D_0 and L_0 represent the width of waveguide and the separation between waveguides, respectively; while n_0 , n_{11} and n_{12} denote the refractive index of cladding and waveguide, respectively. The second term denotes Kerr-type nonlinearity, $I(z, x)$ is the optical intensity, and positive (negative) value of nonlinear coefficient n_2 indicates self-focusing (self-defocusing)

*Electronic address: llz@sxu.edu.cn

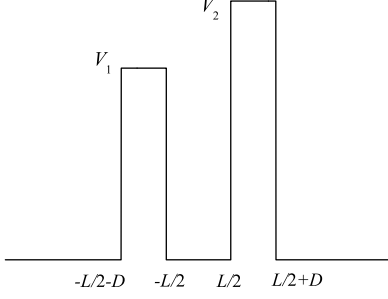


FIG. 1: The profile of a two-channel waveguide with different refractive index.

medium. Under slowly varying envelope approximation, the nonlinear wave equation governing beam propagation in such a waveguide with the refractive index given by Eq. (1) can be written as

$$i \frac{\partial \psi}{\partial z} + \frac{1}{2k_0} \frac{\partial^2 \psi}{\partial x^2} + \frac{k_0 [F(x) - n_0]}{n_0} \psi + \frac{k_0 n_2}{n_0} |\psi|^2 \psi = 0, \quad (2)$$

where $\psi(z, x)$ is the envelope function, and $k_0 = 2\pi n_0/\lambda$ is wave number with λ being wavelength of the optical source generating the beam. By introducing the normalized transformations $\psi(z, x) = (k_0 |n_2| L_D/n_0)^{-1/2} \varphi(\zeta, \xi)$, $\xi = x/w_0$ and $\zeta = z/L_D$ with $L_D = 2k_0 w_0^2$, which represents the diffraction length, we get the dimensionless form of Eq. (2) as follows

$$i \frac{\partial \varphi}{\partial \zeta} + \frac{\partial^2 \varphi}{\partial \xi^2} + V(\xi) \varphi + \eta |\varphi|^2 \varphi = 0, \quad (3)$$

where $\eta = n_2/|n_2| = \pm 1$ corresponds to self-focusing (+) and self-defocusing (-) nonlinearity of the waveguides, respectively, and $V(\xi) = 2k_0^2 w_0^2 [F(w_0 \xi) - n_0]/n_0$ is of the form

$$V(\xi) = \begin{cases} V_1, & -L/2 - D < \xi < -L/2, \\ V_2, & L/2 < \xi < L/2 + D, \\ 0, & \text{otherwise,} \end{cases} \quad (4)$$

which describes the dimensionless two-channel waveguide structure with different refractive index, where $V_1 = 2k_0^2 w_0^2 (n_{11} - n_0)/n_0$ and $V_2 = 2k_0^2 w_0^2 (n_{12} - n_0)/n_0$ being the modulation depth of the refractive index of the left and right waveguide, and $L = L_0/w_0$ and $D = D_0/w_0$ corresponding to scaled separation and width of waveguide, respectively. Here, we use the typical waveguide parameters $D = 3.5$, $L = 5$, $V_2 = 2.525$, and vary V_1 . Figure 1 shows the profile of the two-channel waveguide structure given by Eq. (4). It should be pointed out that such structure can be realized experimentally [38]. It is shown that the Eq. (3) conserves the total energy flow $P(\zeta) = \int_{-\infty}^{+\infty} |\varphi(\zeta, \xi)|^2 d\xi = P_0$, where P_0 is the dimensionless initial total energy.

Assuming that the stationary solution of Eq. (3) is of the form $\varphi(\zeta, \xi) = u(\xi) \exp(i\beta\zeta)$, where $u(\xi)$ is a real

function, and β is the propagation constant, and substituting it into Eq. (3), we find that the function $u(\xi)$ obeys the following nonlinear equation

$$\frac{d^2 u}{d\xi^2} + [V(\xi) - \beta] u + \eta u^3 = 0, \quad (5)$$

where $\eta = \pm 1$ corresponds to self-focusing (+) and self-defocusing (-) nonlinearity of the waveguides, respectively. It should be pointed out that Eq. (5) not only can describe the optical modes in the double-channel waveguide structure with the different refractive index, but also can describe one-dimensional Bose-Einstein condensate trapped in a finite asymmetry double square well potential $-V(\xi)$. In particular, when $V_1 = V_2$, the corresponding optical modes in the symmetric double-channel waveguide structure have been studied, and the results have shown that the coupler not only supports symmetry-preserving modes but also symmetry-breaking modes [36].

III. OPTICAL MODES

In this section, we will present the analytical solutions of Eq. (5) with the potential (4) for $\eta = \pm 1$. Generally, the solutions of Eq. (5) can be constructed in terms of the Jacobi elliptic functions depending on the values of the variable ξ , and have the same propagation constants in different regions. Within the double-channel waveguides of $-L/2 - D < \xi < -L/2$ and $L/2 < \xi < L/2 + D$, the solution of Eq. (5) is the oscillatory function, so it can be selected in the form [37]

$$u_1(\xi; A, K, \delta) = A \operatorname{sn} \left(K\xi + \delta, -\frac{\eta A^2}{2K^2} \right), \quad (6)$$

with $\beta = V_1 - K^2 + \eta A^2/2$ in the region of $-L/2 - D < \xi < -L/2$ and $\beta = V_2 - K^2 + \eta A^2/2$ in the region of $L/2 < \xi < L/2 + D$. In the region of $|\xi| < L/2$, the solution of Eq. (5) has two different Jacobi elliptic functions for the symmetric and the antisymmetric case, respectively. For the symmetric case, the solution is [37]

$$u_2(\xi; B, Q, \sigma) = B \operatorname{nc} \left(Q\xi + \sigma, 1 + \frac{\eta B^2}{2Q^2} \right), \quad (7)$$

with $\beta = Q^2 + \eta B^2$; and for the antisymmetric case, the solution is [37]

$$u_2(\xi; B, Q, \sigma) = B \operatorname{sc} \left(Q\xi + \sigma, 1 + \frac{\eta B^2}{2Q^2} \right), \quad (8)$$

with $\beta = Q^2 - \eta B^2/2$. It should be noted that those two solutions are precise solutions of Eq. (5) for one node and no node within the region of $|\xi| < L/2$. In other regions, the solution of Eq. (5) is required to tend to zero as $\xi \rightarrow \pm\infty$, so it is taken as [36]

$$u_3(\xi; b) = \frac{1}{be^{-\sqrt{\beta}\xi} + ce^{\sqrt{\beta}\xi}}, \quad (9)$$

with $\beta > 0$. Substituting (9) into Eq. (5), one obtains $c = \eta/(8\beta b)$.

Note here that although the modulus in the usual Jacobi elliptic function is restricted from 0 to 1, this problem can be solved by the modular transformation such that the modulus in the Jacobi elliptic functions given by Eqs. (6-8) can take any positive or negative values in our investigations, as shown in Refs. [37, 39], so those solutions do not depend on nonlinearity sign.

In the following, we show the analytical global solutions of Eq. (5). With the help of Eqs. (6), (7) [or (8)], and (9), the solutions of Eq. (5) can be written as

$$u(\xi) = \begin{cases} u_3(\xi; b_1), & \xi < -L/2 - D, \\ u_1(\xi; A_1, K_1, \delta_1), & -L/2 - D < \xi < -L/2, \\ u_2(\xi; B, Q, \sigma), & |\xi| < L/2, \\ u_1(\xi; A_2, K_2, \delta_2), & L/2 < \xi < L/2 + D, \\ u_3(\xi; b_2), & \xi > L/2 + D. \end{cases} \quad (10)$$

The continuity conditions for u and $\partial u/\partial \xi$ at the boundaries of $\xi = \pm L/2$ and $\xi = \pm(L/2 + D)$ require

$$\begin{aligned} u_3(-L/2 - D; b_1) &= u_1(-L/2 - D; A_1, K_1, \delta_1), \\ \frac{du_3}{d\xi}(-L/2 - D; b_1) &= \frac{du_1}{d\xi}(-L/2 - D; A_1, K_1, \delta_1), \\ u_1(-L/2; A_1, K_1, \delta_1) &= u_2(-L/2; B, Q, \sigma), \\ \frac{du_1}{d\xi}(-L/2; A_1, K_1, \delta_1) &= \frac{du_2}{d\xi}(-L/2; B, Q, \sigma), \\ u_2(L/2; B, Q, \sigma) &= u_1(L/2; A_2, K_2, \delta_2), \\ \frac{du_2}{d\xi}(L/2; B, Q, \sigma) &= \frac{du_1}{d\xi}(L/2; A_2, K_2, \delta_2), \\ u_1(L/2 + D; A_2, K_2, \delta_2) &= u_3(L/2 + D; b_2), \\ \frac{du_1}{d\xi}(L/2 + D; A_2, K_2, \delta_2) &= \frac{du_3}{d\xi}(L/2 + D; b_2), \end{aligned} \quad (11)$$

with $\beta = V_1 - K_1^2 + \eta A_1^2/2 = V_2 - K_2^2 + \eta A_2^2/2$, and $\beta = Q^2 + \eta B^2$ for the symmetric case given by Eq. (7) or $\beta = Q^2 - \eta B^2/2$ for the antisymmetric case given by Eq. (8). In Eq. (10), there are eleven parameters $A_1, K_1, \delta_1, A_2, K_2, \delta_2, B, Q, \sigma, b_1$, and b_2 , which can be calculated by solving numerically Eqs. (11) with the conditions that the propagation constants in different regions should be same. Once those parameters are determined numerically, we can obtain the exact optical modes for asymmetric double-channel nonlinear waveguides.

Fig. 2 and Fig. 3 show several different optical modes in a nonlinear asymmetric double-channel waveguide in the self-defocusing medium and the self-focusing medium, respectively. These optical modes are induced from the symmetry-preserving optical modes in the symmetric double-channel waveguide, where for comparison, we also plotted the corresponding symmetry-preserving optical modes in the symmetric double-channel waveguides in the same figure. From Figs. 2 and 3, we found that the symmetry of the modes is broken due to asymmetry of the two-channel waveguide, and the amplitude of the modes in the lower refractive index waveguide is

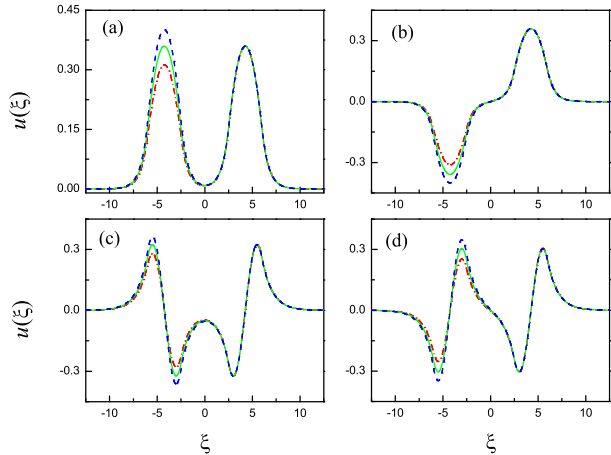


FIG. 2: (Color Online) Various different optical modes existing in self-defocusing medium ($\eta = -1$), where the dash-dotted red line is the optical mode for $V_1 = 2.500$, the solid green line is the optical mode for $V_1 = 2.525$, and the dashed blue line is the optical mode for $V_1 = 2.550$. Here $\beta = 2.00$ in (a) and (b), $\beta = 0.85$ in (c) and (d).

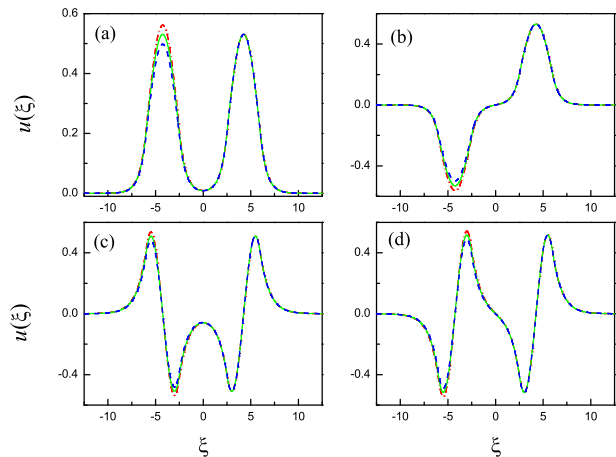


FIG. 3: (Color Online) Various different optical modes existing in self-focusing medium ($\eta = 1$), where the dash-dotted red line is the optical mode for $V_1 = 2.500$, the solid green line is the optical mode for $V_1 = 2.525$, and the dashed blue line is the optical mode for $V_1 = 2.550$. Here $\beta = 2.30$ in (a) and (b), $\beta = 1.10$ in (c) and (d).

smaller than that in the higher refractive index waveguide for the self-defocusing medium, while for the self-focusing medium, the amplitude of the modes in the lower refractive index waveguide is larger than that in the higher refractive index waveguide.

We also demonstrate the profiles of optical modes with dependence on the propagation constant β . Fig. 4 and Fig. 5 present several corresponding modes shown in

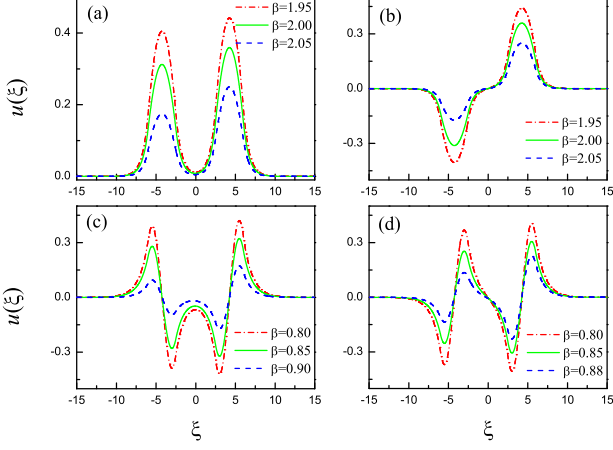


FIG. 4: (Color Online) Several optical modes with different β in a nonlinear asymmetrical double-channel waveguide for the self-defocusing medium ($\eta = -1$). Here the parameters are $V_1 = 2.500$ and $V_2 = 2.525$.

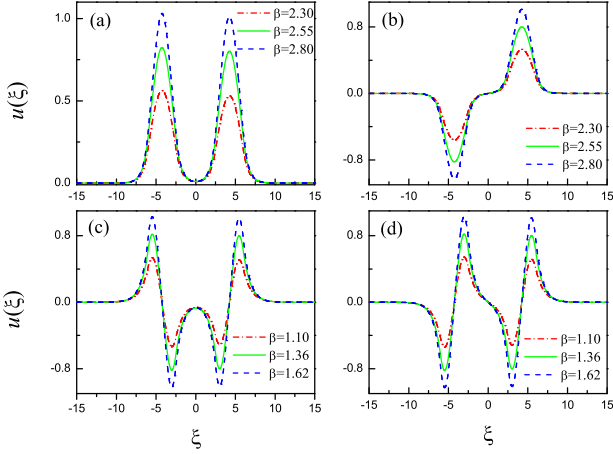


FIG. 5: (Color Online) Several optical modes with different β in a nonlinear asymmetrical double-channel waveguide for the self-focusing medium ($\eta = 1$). Here the parameters are the same as in Fig. 4.

Figs. 2 and 3 for different propagation constant β . From them, one can see that, for self-defocusing media the profile of nonlinear modes is shrunk, and the corresponding amplitude becomes smaller with an increase of the propagation constant β , while for self-focusing case it is opposite, namely, the profile of nonlinear modes becomes more prominent and the corresponding amplitude becomes larger. This feature can be depicted by the dispersion relations between the total energy P_0 and the propagation constant β . As shown in Fig. 8 and Fig. 9, one can see that the total energy decreases with the increase of the propagation constant for self-defocusing

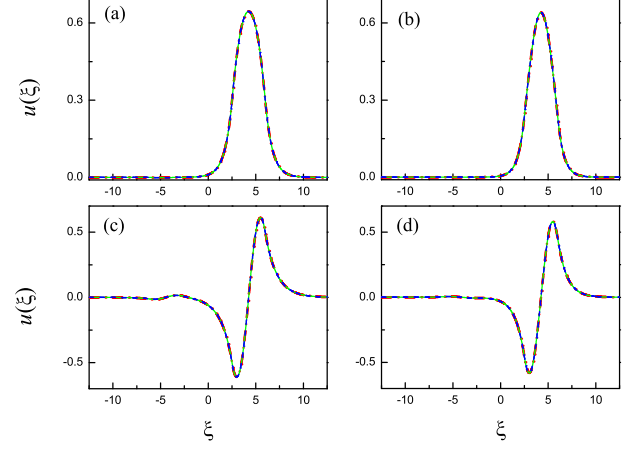


FIG. 6: (Color Online) Several symmetry-breaking optical modes, where the dash-dotted red lines are optical modes for $V_1 = 2.500$, the solid green lines are optical modes for $V_1 = 2.525$, and the dashed blue lines are optical modes for $V_1 = 2.550$. Here $\eta = -1$ in (a) and (c), $\eta = 1$ in (b) and (d) and $\beta = 1.78$ in (a), $\beta = 2.39$ in (b), $\beta = 0.66$ in (c) and $\beta = 1.15$ in (d).

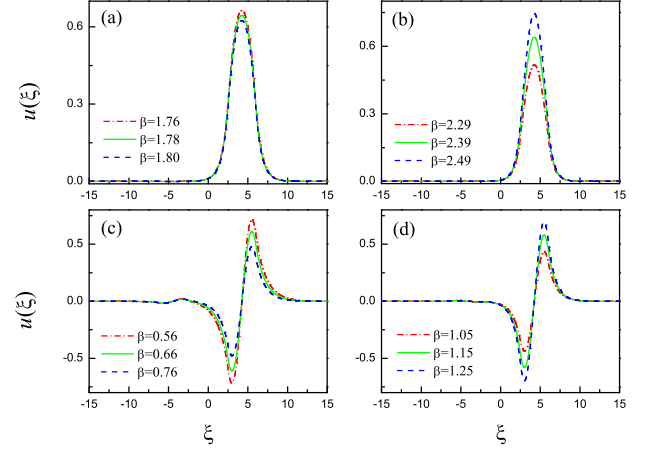


FIG. 7: (Color Online) Several symmetry-breaking optical modes with different β in a nonlinear asymmetrical double-channel waveguide. Here the parameters are the same as in Fig. 6.

media (see Fig. 8), whereas it is an increasing function of the propagation constant for self-focusing case (see Fig. 9).

As discussed in Ref. [36], besides the symmetry-preserving optical modes, a double-channel waveguide also supports the symmetry-breaking optical modes, and the corresponding optical modes in a nonlinear asymmetrical double-channel waveguide are presented in Fig. 6, in which we also plotted the corresponding symmetry-

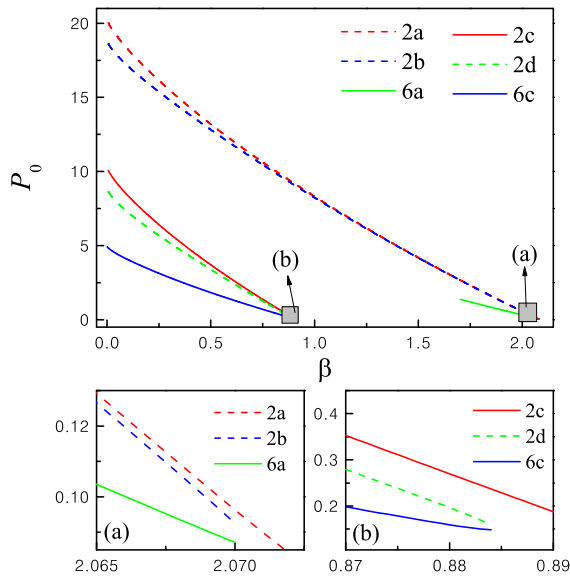


FIG. 8: (Color Online) The dependence of the total energy P_0 on the propagation constant β for the modes existing in self-defocusing medium ($\eta = -1$). Here the parameters are $V_1 = 2.500$ and $V_2 = 2.525$. The labeled shadow areas are enlarged in corresponding (a)-(b). And the labels 2a, 2b, \dots , mean the corresponding modes shown in Fig. 2a, 2b, \dots , respectively.

breaking optical modes in a symmetric double-channel waveguide in the same figure for comparison. One can find that the optical modes in a nonlinear asymmetric double-channel waveguide are almost the same as the modes in a symmetric one for the given β .

Similarly, the corresponding modes shown in Fig. 6 for different propagation constant β are presented in Fig. 7. It is shown that the profile of nonlinear modes becomes shrunk with the increase of the propagation constant β for the self-defocusing case, while for the self-focusing case the profile of nonlinear modes becomes more pronounced. This feature is depicted by the dispersion relations between the total energy P_0 and the propagation constant β . It should be pointed out that the modes shown in Fig. 6 only exist in a small region, as shown in Fig. 8 and Fig. 9.

From the dispersion relations shown in Figs. 8 and 9, one can see that for the self-defocusing medium there is no intersection between dispersion curves (see Fig. 8 and the enlarged Figs. 8a and 8b), which indicates that there is no degenerate modes existing, and the total energy of the mode shown in Fig. 2a is the highest for a given propagation constant β . While for the self-focusing medium the dispersion curves can intersect (see the enlarged Figs. 9c and 9d), which implies that there exists two different modes with the same total energy at the intersection point, namely, the degeneracy occurs at the intersection point. Note that for our choices of the pa-

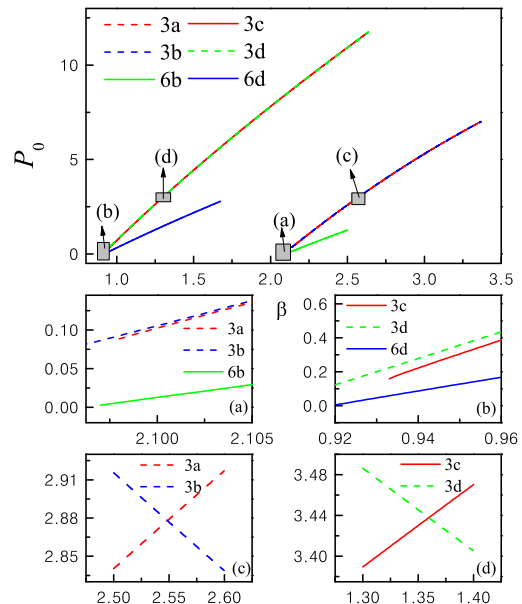


FIG. 9: (Color Online) The dependence of the total energy P_0 on the propagation constant β for the modes existing in self-focusing medium ($\eta = 1$). Here the parameters are $V_1 = 2.500$ and $V_2 = 2.525$. The labeled shadow areas are enlarged in corresponding (a)-(d). And the labels 3a, 3b, \dots , mean the corresponding modes shown in Fig. 3a, 3b, \dots , respectively.

rameters, the intersection points of the dispersion curves for the modes shown in Figs. 3a and 3b, and Figs. 3c and 3d are about 2.5485 and 1.3595, respectively, and the corresponding degenerate modes are shown by the green solid curves in Fig. 5. Here, to distinguish the case of the intersection, we rotate the dispersion curve for the modes shown in Fig. 3a (Fig. 3c) for an angle of $\pi/6$ anticlockwise as the center of intersection point and the same angle for dispersion curve of the mode shown in Fig. 3b (Fig. 3d) but rotate clockwise, as shown in Figs. 9c and 9d.

IV. THE NONLINEAR MANIPULATION OF OPTICAL MODES IN DOUBLE-CHANNEL WAVEGUIDE

In this section, we will demonstrate the control and manipulation of optical modes in reconfigurable nonlinear media. Thus our interest is to investigate the evolution dynamics of optical beams existing in double-channel waveguide propagating into a uniform nonlinear medium. In this case, the governing equation can be generally written as

$$i \frac{\partial \psi}{\partial z} + \frac{1}{2k_0} \frac{\partial^2 \psi}{\partial x^2} + \frac{k_0 \Delta n(z, x)}{n_0} \psi = 0, \quad (12)$$

where the refractive index change $\Delta n(z, x)$ is a function of z and x , and $\Delta n(z, x) = n(z, x) - n_0$. Here we assume

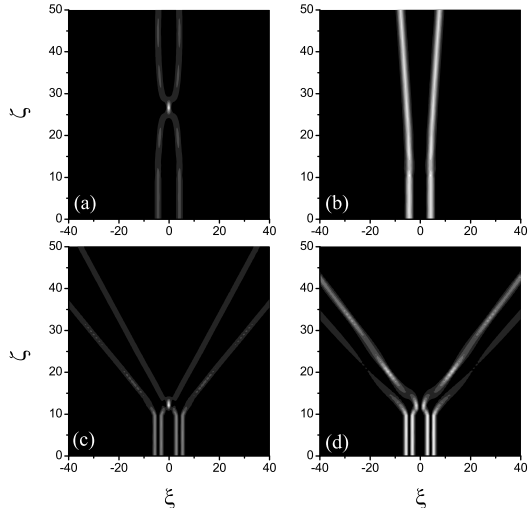


FIG. 10: (Color Online) The evolution of optical modes shown in Fig. 2 into the self-focusing Kerr medium without channels, where $\eta' = 10$ in (a) and (b), and $\eta' = 20$ in (c) and (d). Here the parameters are $V_1 = V_2 = 2.525$ and $\zeta_0 = 10$. The labels (a), (b), (c), and (d) mean the corresponding modes shown in Fig. 2a, 2b, 2c, and 2d, respectively.

that when $0 \leq z \leq Z_0$, $n(z, x)$ is in the form of Eq. (1), $\Delta n(z, x) = F(x) + n_2 I(z, x) - n_0$; while for $z > Z_0$, $\Delta n(z, x) = n'_2 I(z, x) - n_0$. Here, n_2 and n'_2 are the Kerr nonlinear coefficients of different media in the region of $0 \leq z \leq Z_0$ and $z > Z_0$, respectively. Thus, when $0 \leq z \leq Z_0$, namely in the region of $0 \leq \zeta \leq \zeta_0$, Eq. (12) can be normalized to Eq. (3), where $\zeta = z/L_D$ and $\zeta_0 = Z_0/L_D$ with $L_D = 2k_0 w_0^2$. At the same time, in the region of $z > Z_0$, namely $\zeta > \zeta_0$, Eq. (12) is reduced to the dimensionless form as follows

$$i \frac{\partial \varphi}{\partial \zeta} + \frac{\partial^2 \varphi}{\partial \xi^2} + \eta' |\varphi|^2 \varphi = 0, \quad (13)$$

where $\eta' = n'_2/|n_2|$. Note that Eq. (13) is different from Eq. (3), in which Eq. (3) includes a potential function $V(\xi)$ given by Eq. (4), while Eq. (13) does not include and can describe the dynamics of beams in Kerr media without any refractive index modulation.

In the following analysis, optical beams of different modes existing in double-channel waveguide are injected into the uniform nonlinear medium after propagating diffraction length of ζ_0 in double-channel waveguide.

First we consider the situation that optical beams are injected from symmetrical double-channel waveguide. For the optical modes shown in Fig. 2, which exist in self-defocusing medium ($\eta = -1$), the numerical simulations show that when $\eta' < 0$, these optical modes are diffracted quickly after entering into a uniform Kerr medium. However, when $\eta' > 0$ and is large enough, the evolution of optical beams exhibits different scenarios in the Kerr medium without any channels, as shown in Fig.

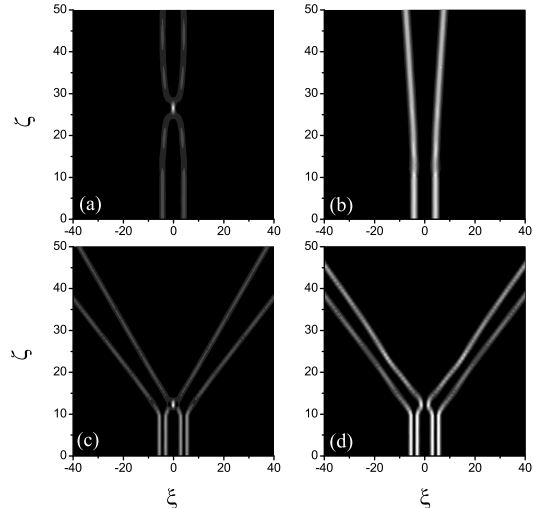


FIG. 11: (Color Online) The evolution of optical modes shown in Fig. 3 into the self-focusing Kerr medium without channels, where $\eta' = 5$ in (a) and (b), and $\eta' = 10$ in (c) and (d). Here the parameters are $V_1 = V_2 = 2.525$ and $\zeta_0 = 10$. The labels (a), (b), (c), and (d) mean the corresponding modes shown in Fig. 3a, 3b, 3c, and 3d, respectively.

10. Similarly, for the optical modes shown in Fig. 3, which exist in self-focusing media ($\eta = 1$) with double-channel waveguide, as shown in Fig. 11, our numerical simulations show that the evolution of optical modes exhibit almost similar properties with that in Fig. 10.

From Figs. 10 and 11, one can see that when the optical modes existing both in self-defocusing and self-focusing media with double-channel waveguide are injected into the self-defocusing medium without any channels, the beams should be diffracted quickly. However, when the optical modes are injected into the self-focusing medium without any channels and the corresponding nonlinear coefficient η' is enough larger, the beams could be manipulated effectively. In this situation, when the optical modes shown in Fig. 2a and Fig. 3a are injected into self-focusing medium without any channels the beams appear to attract and repel each other periodically, as shown in Figs. 10a and 11a. While when the modes shown in Figs. 2b-2d and Figs. 3b-3d are injected into self-focusing medium without any channels, the beams repel each other, as shown in Figs. 10b-10d and Figs. 11b-11d. Note that the escape angle are the same for the beams in Fig. 2b (Fig. 3b) due to the symmetry of the double-channel waveguide.

The evolution of optical modes shown in Fig. 6 is presented in Fig. 12, in which Figs. 12a and 12c (Figs. 12b and 12d) demonstrate the evolution of optical modes in the self-focusing medium without any channels with initial input beams injected from self-defocusing (self-focusing) medium with double-channel waveguide. As shown in Fig. 12a and 12b, one can see that optical

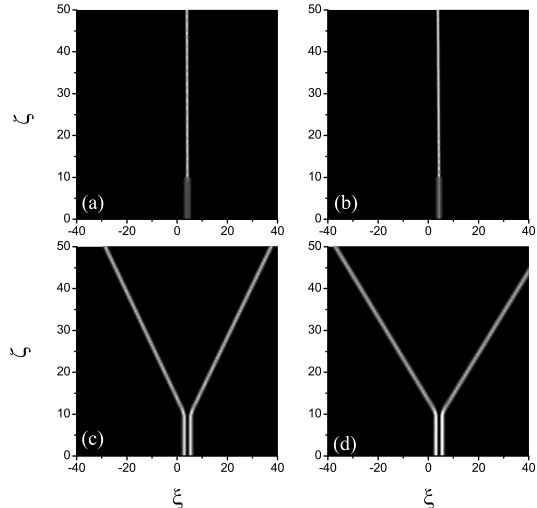


FIG. 12: (Color Online) The evolution of optical modes shown in Fig. 6 into the self-focusing Kerr medium without channels, where $\eta' = 10$. Here the parameters are $V_1 = V_2 = 2.525$ and $\zeta_0 = 10$. The labels (a), (b), (c), and (d) mean the corresponding modes shown in Fig. 6a, 6b, 6c, and 6d, respectively.

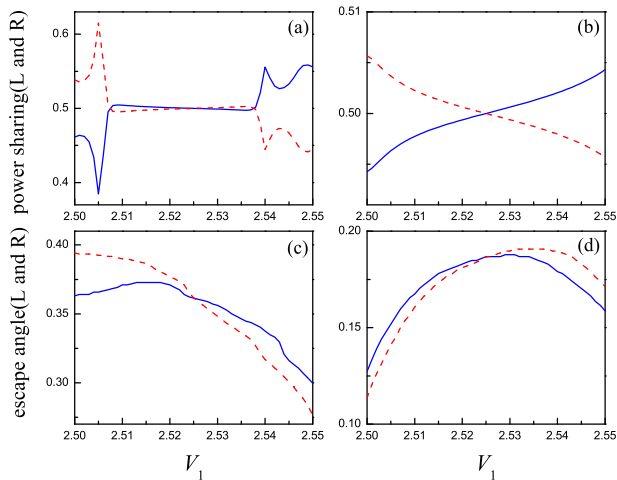


FIG. 13: (Color Online) Energy sharing (row 1) and escape angles (row 2) of optical beams as a function of parameter V_1 . In all cases, the solid-blue and the dashed-red curves correspond to the left and right beams, respectively. Here the parameter are $V_2 = 2.525$, $\eta' = 10$ in (a) and (c) corresponding to the modes shown in Fig. 2b (namely Fig. 11b) and $\eta' = 5$ in (b) and (d) corresponding to the modes shown in Fig. 3b (namely Fig. 12b).

beams with a single hump can be compressed effectively, and as shown in Figs. 12c and 12d the optical modes with two peaks are separated during the evolution due to the repulsive interaction force resulted from the phase difference between the two peaks.

It should be pointed out that these results only take into account the optical modes existing in the symmetrical double-channel waveguide. Then, one will naturally ask what is the influence of the asymmetrical double-channel on the evolution of optical modes. In order to understand this question, we launch optical beams from an asymmetrical double-channel waveguide into the self-focusing medium to observe their evolution by tuning the depth of left channel of the waveguide for a fixed depth of the right channel, namely, the value of V_1 varies from 2.500 to 2.550 for $V_2 = 2.525$. As an example, we demonstrated the evolution dynamics for the modes shown in Fig. 2b and Fig. 3b. In Fig. 13, we present the dependence of the energy sharing, the ratio of the energy carried by each component in the mode over the total energy, and the escape angle, the angle of the each peak in the mode and the propagation direction ζ , on the value of V_1 . As shown in Fig. 13, one can see that the energy carried by each beam is different due to the asymmetry of the double-channel waveguide [shown in Figs. 13a and 13b]. Also, one can see clearly that the escape angles of the two beams take different values with the change of the value V_1 , which means that the beams can be controlled by tuning the depth of the left channel of the waveguide.

V. CONCLUSION

We have studied light beam propagation in an asymmetric double-channel waveguide in the form of a nonlinear coupler. A family of analytical solutions with symmetric and antisymmetric forms has been obtained for both self-focusing and self-defocusing nonlinear media, and the dispersion relations between the total energy and the propagation constant has been discussed in detail. Our results reveal that the system with self-focusing nonlinear response supports the degenerate modes, while for self-defocusing medium the degenerate modes do not exist. In addition, we explored new ways to steer optical modes propagating from double-channel waveguide into a uniform self-focusing medium. The compression of beam with single hump and split of beams with two humps have been demonstrated by tuning the depth of the channel of the waveguide. These properties may be applied in practical optical devices, and be useful for optical processing, optical switching or optical routing.

VI. ACKNOWLEDGEMENT

The authors acknowledge fruitful discussions with Professor Yuri Kivshar. This research is supported by the National Natural Science Foundation of China grant 61078079, the Shanxi Scholarship Council of China grant 2011-010, and the Australian Research Council.

-
- [1] S. Longhi, *Laser Photon. Rev.* **3**, 243 (2009).
- [2] W. J. Tomlinson, *Opt. Lett.* **5**, 323 (1980).
- [3] V. K. Fedyanin and D. Mihalache, *Z. Phys. B* **47**, 167 (1982); D. Mihalache, R. G. Nazmitdinov, and V. K. Fedyanin, *Physica Scripta* **29**, 269 (1984); D. Mihalache, D. Mazilu, and H. Totia, *Physica Scripta* **30**, 335 (1984).
- [4] N. N. Akhmediev, *Zh. Eksp. Teor. Fiz.* **83**, 545 (1982) [*Sov. Phys. JETP* **56**, 299 (1982)].
- [5] G. I. Stegeman, C. T. Seaton, J. Chilwell, and S. D. Smith, *Appl. Phys. Lett.* **44**, 830 (1984).
- [6] N. N. Akhmediev, V. I. Korneyev, and Y. V. Kuzmenko, *Zh. Eksp. Teor. Fiz.* **88**, 107 (1985).
- [7] F. Lederer and D. Mihalache, *Solid State Commun.* **59**, 151 (1986); D. Mihalache, D. Mazilu, and F. Lederer, *Opt. Commun.* **59**, 391 (1986).
- [8] D. Mihalache, G. I. Stegeman, C. T. Seaton, E. M. Wright, R. Zononi, A. D. Boardman, and T. Twardowski, *Opt. Lett.* **12**, 187 (1987).
- [9] D. Mihalache, M. Bertolotti, and C. Sibilina, *Prog. Opt.* **27**, 229 (1989).
- [10] U. Langbein, F. Lederer, T. Peschel, U. Trutschel, and D. Mihalache, *Phys. Reports* **194**, 325 (1990).
- [11] A. D. Boardman, P. Egan, U. Langbein, F. Lederer, and D. Mihalache, in “Nonlinear surface electromagnetic phenomena”, Edited by H. E. Ponath and G. I. Stegeman, North-Holland, Amsterdam, 1991, pp. 73-287.
- [12] F. Lederer, L. Leine, R. Muschall, T. Peschel, C. Schmidt-Hattenberger, U. Trutschel, A. D. Boardman, C. Wächter, *Opt. Commun.* **99**, 95 (1993).
- [13] A. R. Davoyan, I. V. Shadrivov, and Y. S. Kivshar, *Opt. Express* **16**, 21209 (2008).
- [14] D. Marcuse, *Journal of Lightwave Technology* **5**, 113 (1987).
- [15] C. C. Yang, *Opt. Lett.* **16**, 1641 (1991).
- [16] C. C. Yang and A. J. S. Wang, *IEEE Journal of Quantum Electronics* **28**, 479 (1992).
- [17] Y. Chen, *Optical and Quantum Electronics* **24**, 539 (1992).
- [18] K. Yasumoto, H. Maeda, and N. Maekawa, *Journal of Lightwave Technology* **14**, 628 (1996).
- [19] D. N. Christodoulides, F. Lederer, and Y. Silberberg, *Nature (London)* **424**, 817 (2003).
- [20] F. Lederer, G. I. Stegeman, D. N. Christodoulides, G. Asanto, M. Segev, Y. Silberberg, *Phys. Rep.* **463**, 1 (2008).
- [21] Y. V. Kartashov, V. A. Vysloukh, and L. Torner, *Prog. Opt.* **52**, 63 (2009).
- [22] H. S. Eisenberg, Y. Silberberg, R. Morandotti, A. R. Boyd, and J. S. Aitchison, *Phys. Rev. Lett.* **81**, 3383 (1998); D. Mandelik, H. S. Eisenberg, Y. Silberberg, R. Morandotti, and J. S. Aitchison, *Phys. Rev. Lett.* **90**, 053902 (2003).
- [23] M. J. Ablowitz and Z. H. Musslimani, *Phys. Rev. Lett.* **87**, 254102 (2001).
- [24] Y. Lahini, E. Frumker, Y. Silberberg, S. Droulias, K. Hizanidis, R. Morandotti, and D. N. Christodoulides, *Phys. Rev. Lett.* **98**, 023901 (2007).
- [25] J. W. Fleischer, M. Segev, N. K. Efremidis, and D. N. Christodoulides, *Nature (London)* **422**, 147 (2003); J. W. Fleischer, T. Carmon, M. Segev, N. K. Efremidis, and D. N. Christodoulides, *Phys. Rev. Lett.* **90**, 023902 (2003).
- [26] D. Neshev, E. Ostrovskaya, Y. Kivshar, and W. Krolikowski, *Opt. Lett.* **28**, 710 (2003).
- [27] Y. V. Kartashov, V. A. Vysloukh, and L. Torner, *Phys. Rev. Lett.* **93**, 153903 (2004).
- [28] Y. P. Zhang and B. Wu, *Phys. Rev. Lett.* **102**, 093905 (2009).
- [29] J. Proctor and J. Kutz, *Opt. Lett.* **30**, 2013 (2005).
- [30] A. B. Aceves, T. Peschel, R. Muschall, F. Lederer, S. Trillo, and S. Wabnitz, *Phys. Rev. E* **53**, 1172 (1996).
- [31] H. F. Zhang, J. Jia, S. T. Jia, and L. Li, *Opt. Commun.* **281**, 4130 (2008).
- [32] Z. Xu, Mario I. Molina, and Yuri S. Kivshar, *Phys. Rev. A* **80**, 013817 (2009).
- [33] Y. V. Kartashov, B. A. Malomed, and L. Torner, *Rev. Mod. Phys.* **83**, 247 (2011).
- [34] P. G. Kevrekidis, Zhigang Chen, B. A. Malomed, D. J. Frantzeskakis, and M. I. Weinstein, *Phys. Lett. A* **340**, 275 (2005).
- [35] Ze'ev Birnbaum and B. A. Malomed, *Physica D* **237**, 3252 (2008).
- [36] J. F. Jia, Y. P. Zhang, W. D. Li, and L. Li, *Opt. Commun.* **283**, 132 (2010).
- [37] W. D. Li, *Phys. Rev. A* **74**, 063612 (2006).
- [38] T. Pertsch, P. Dannberg, W. Elflein, A. Brauer, and F. Lederer, *Phys. Rev. Lett.* **83**, 4752 (1999).
- [39] P. F. Byrd and M. D. Friedman, *Handbook of Elliptic Integrals for Engineers and Scientists*, 2nd ed. Springer-Verlag, New York, 1971.